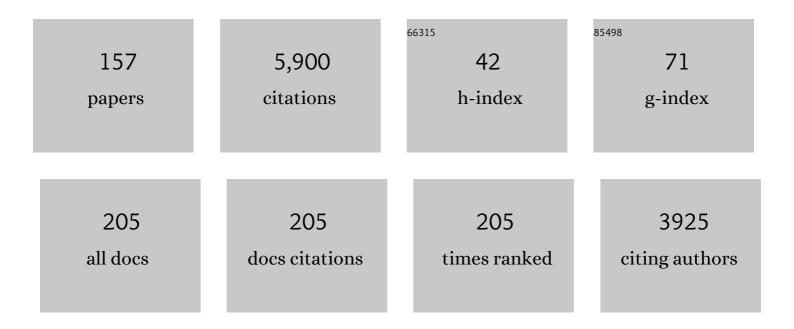
Matteo Massironi

List of Publications by Year in descending order

Source: https://exaly.com/author-pdf/6107939/publications.pdf Version: 2024-02-01



#	Article	lF	CITATIONS
1	On the nucleus structure and activity of comet 67P/Churyumov-Gerasimenko. Science, 2015, 347, aaa1044.	6.0	366
2	The morphological diversity of comet 67P/Churyumov-Gerasimenko. Science, 2015, 347, aaa0440.	6.0	259
3	Images of Asteroid 21 Lutetia: A Remnant Planetesimal from the Early Solar System. Science, 2011, 334, 487-490.	6.0	179
4	Geological outline of the Alps. Episodes, 2003, 26, 175-180.	0.8	177
5	The primordial nucleus of comet 67P/Churyumov-Gerasimenko. Astronomy and Astrophysics, 2016, 592, A63.	2.1	159
6	Large heterogeneities in comet 67P as revealed by active pits from sinkhole collapse. Nature, 2015, 523, 63-66.	13.7	158
7	Regional surface morphology of comet 67P/Churyumov-Gerasimenko from Rosetta/OSIRIS images. Astronomy and Astrophysics, 2015, 583, A26.	2.1	153
8	A NEW CHRONOLOGY FOR THE MOON AND MERCURY. Astronomical Journal, 2009, 137, 4936-4948.	1.9	152
9	Redistribution of particles across the nucleus of comet 67P/Churyumov-Gerasimenko. Astronomy and Astrophysics, 2015, 583, A17.	2.1	149
10	Two independent and primitive envelopes of the bilobate nucleus of comet 67P. Nature, 2015, 526, 402-405.	13.7	141
11	Evidence for Young Volcanism on Mercury from the Third MESSENGER Flyby. Science, 2010, 329, 668-671.	6.0	118
12	Laser scanning-based recognition of rotational movements on a deep seated gravitational instability: The Cinque Torri case (North-Eastern Italian Alps). Geomorphology, 2010, 122, 191-204.	1.1	113
13	Gravitational slopes, geomorphology, and material strengths of the nucleus of comet 67P/Churyumov-Gerasimenko from OSIRIS observations. Astronomy and Astrophysics, 2015, 583, A32.	2.1	113
14	Summer fireworks on comet 67P. Monthly Notices of the Royal Astronomical Society, 2016, 462, S184-S194.	1.6	112
15	The Colour and Stereo Surface Imaging System (CaSSIS) for the ExoMars Trace Gas Orbiter. Space Science Reviews, 2017, 212, 1897-1944.	3.7	111
16	Size-frequency distribution of boulders ≥7 m on comet 67P/Churyumov-Gerasimenko. Astronomy and Astrophysics, 2015, 583, A37.	2.1	108
17	Are fractured cliffs the source of cometary dust jets? Insights from OSIRIS/Rosetta at 67P/Churyumov-Gerasimenko. Astronomy and Astrophysics, 2016, 587, A14.	2.1	102
18	The pristine interior of comet 67P revealed by the combined Aswan outburst and cliff collapse. Nature Astronomy, 2017, 1, .	4.2	100

#	Article	IF	CITATIONS
19	Rosetta's comet 67P/Churyumov-Gerasimenko sheds its dusty mantle to reveal its icy nature. Science, 2016, 354, 1566-1570.	6.0	97
20	Regional surface morphology of comet 67P/Churyumov-Gerasimenko from Rosetta/OSIRIS images: The southern hemisphere. Astronomy and Astrophysics, 2016, 593, A110.	2.1	86
21	Lava tubes on Earth, Moon and Mars: A review on their size and morphology revealed by comparative planetology. Earth-Science Reviews, 2020, 209, 103288.	4.0	80
22	Fractures on comet 67P/Churyumovâ€Gerasimenko observed by Rosetta/OSIRIS. Geophysical Research Letters, 2015, 42, 5170-5178.	1.5	71
23	SIMBIO-SYS: The spectrometer and imagers integrated observatory system for the BepiColombo planetary orbiter. Planetary and Space Science, 2010, 58, 125-143.	0.9	70
24	Scientific assessment of the quality of OSIRIS images. Astronomy and Astrophysics, 2015, 583, A46.	2.1	67
25	Detection of exposed H ₂ O ice on the nucleus of comet 67P/Churyumov-Gerasimenko. Astronomy and Astrophysics, 2016, 595, A102.	2.1	67
26	Interpretation and processing of ASTER data for geological mapping and granitoids detection in the Saghro massif (eastern Anti-Atlas, Morocco). , 2008, 4, 736.		66
27	Temporal morphological changes in the Imhotep region of comet 67P/Churyumov-Gerasimenko. Astronomy and Astrophysics, 2015, 583, A36.	2.1	60
28	Geomorphology of the Imhotep region on comet 67P/Churyumov-Gerasimenko from OSIRIS observations. Astronomy and Astrophysics, 2015, 583, A35.	2.1	59
29	The geomorphology of (21) Lutetia: Results from the OSIRIS imaging system onboard ESA's Rosetta spacecraft. Planetary and Space Science, 2012, 66, 96-124.	0.9	58
30	3D fold and fault reconstruction with an uncertainty model: An example from an Alpine tunnel case study. Computers and Geosciences, 2008, 34, 351-372.	2.0	57
31	Mapping the Buraburi granite in the Himalaya of Western Nepal: Remote sensing analysis in a collisional belt with vegetation cover and extreme variation of topography. Remote Sensing of Environment, 2011, 115, 1129-1144.	4.6	57
32	The Aosta–Ranzola extensional fault system and Oligocene–Present evolution of the Austroalpine–Penninic wedge in the northwestern Alps. International Journal of Earth Sciences, 2001, 90, 654-667.	0.9	56
33	Comet 67P/Churyumov-Gerasimenko: Constraints on its origin from OSIRIS observations. Astronomy and Astrophysics, 2015, 583, A44.	2.1	53
34	Aswan site on comet 67P/Churyumov-Gerasimenko: Morphology, boulder evolution, and spectrophotometry. Astronomy and Astrophysics, 2016, 592, A69.	2.1	53
35	The effects of the target material properties and layering on the crater chronology: The case of Raditladi and Rachmaninoff basins on Mercury. Planetary and Space Science, 2011, 59, 1968-1980.	0.9	51
36	SIMBIO-SYS: Scientific Cameras and Spectrometer for the BepiColombo Mission. Space Science Reviews, 2020, 216, 1.	3.7	47

#	Article	IF	CITATIONS
37	Post-nappe brittle tectonics and kinematic evolution of the north-western Alps: an integrated approach. Tectonophysics, 2000, 327, 267-292.	0.9	46
38	The cratering history of asteroid (2867) Steins. Planetary and Space Science, 2010, 58, 1116-1123.	0.9	46
39	Volcanism and tectonism across the inner solar system: an overview. Geological Society Special Publication, 2015, 401, 1-56.	0.8	46
40	Rationale for BepiColombo Studies of Mercury's Surface and Composition. Space Science Reviews, 2020, 216, 1.	3.7	46
41	The scattering phase function of comet 67P/Churyumov–Gerasimenko coma as seen from the Rosetta/OSIRIS instrument. Monthly Notices of the Royal Astronomical Society, 2017, 469, S404-S415.	1.6	44
42	Average strain rate in the Italian crust inferred from a permanent GPS network - II. Strain rate versus seismicity and structural geology. Geophysical Journal International, 2003, 155, 254-268.	1.0	43
43	Three-dimensional characterization of a crustal-scale fault zone: The Pusteria and Sprechenstein fault system (Eastern Alps). Journal of Structural Geology, 2010, 32, 2022-2041.	1.0	43
44	The cratering history of asteroid (21) Lutetia. Planetary and Space Science, 2012, 66, 87-95.	0.9	43
45	Seasonal erosion and restoration of the dust cover on comet 67P/Churyumov-Gerasimenko as observed by OSIRIS onboard Rosetta. Astronomy and Astrophysics, 2017, 604, A114.	2.1	43
46	Geological map and stratigraphy of asteroid 21 Lutetia. Planetary and Space Science, 2012, 66, 125-136.	0.9	42
47	The Latemar: A Middle Triassic polygonal fault-block platform controlled by synsedimentary tectonics. Sedimentary Geology, 2011, 234, 1-18.	1.0	41
48	Physical properties of craters on asteroid (21) Lutetia. Planetary and Space Science, 2012, 66, 79-86.	0.9	41
49	Geomorphology and spectrophotometry of Philae's landing site on comet 67P/Churyumov-Gerasimenko. Astronomy and Astrophysics, 2015, 583, A41.	2.1	41
50	The pebbles/boulders size distributions on Sais: Rosetta's final landing site on comet 67P/Churyumov–Gerasimenko. Monthly Notices of the Royal Astronomical Society, 2017, 469, S636-S645.	1.6	40
51	Mercury's radius change estimates revisited using MESSENGER data. Icarus, 2012, 221, 456-460.	1.1	39
52	Meter-scale thermal contraction crack polygons on the nucleus of comet 67P/Churyumov-Gerasimenko. Icarus, 2018, 301, 173-188.	1.1	33
53	Mercury's surface and composition to be studied by BepiColombo. Planetary and Space Science, 2010, 58, 21-39.	0.9	31
54	Misoriented faults in exhumed metamorphic complexes: Rule or exception?. Earth and Planetary Science Letters, 2011, 307, 233-239.	1.8	31

#	Article	IF	CITATIONS
55	(21) Lutetia spectrophotometry from Rosetta-OSIRIS images and comparison to ground-based observations. Planetary and Space Science, 2012, 66, 43-53.	0.9	31
56	The highly active Anhur–Bes regions in the 67P/Churyumov–Gerasimenko comet: results from OSIRIS/ROSETTA observations. Monthly Notices of the Royal Astronomical Society, 2017, 469, S93-S107.	1.6	30
57	Miocene to Present kinematics of the NW-Alps: evidences from remote sensing, structural analysis, seismotectonics and thermochronology. Journal of Geodynamics, 2000, 30, 205-228.	0.7	29
58	Use of PSInSARâ,,¢ data to infer active tectonics: Clues on the differential uplift across the Giudicarie belt (Central-Eastern Alps, Italy). Tectonophysics, 2009, 476, 297-303.	0.9	28
59	Beagle Rupes – Evidence for a basal decollement of regional extent in Mercury's lithosphere. Icarus, 2010, 209, 256-261.	1.1	27
60	Geologic mapping of the Comet 67P/Churyumov–Gerasimenko's Northern hemisphere. Monthly Notices of the Royal Astronomical Society, 2016, 462, S352-S367.	1.6	27
61	The southern hemisphere of 67P/Churyumov-Gerasimenko: Analysis of the preperihelion size-frequency distribution of boulders ≥7 m. Astronomy and Astrophysics, 2016, 592, L2.	2.1	27
62	Dating deformation in the Gran Paradiso Massif (NW Italian Alps): Implications for the exhumation of high-pressure rocks in a collisional belt. Lithos, 2012, 144-145, 130-144.	0.6	26
63	Phobos grooves and impact craters: A stereographic analysis. Icarus, 2015, 256, 90-100.	1.1	26
64	Characterization of the Abydos region through OSIRIS high-resolution images in support of CIVA measurements. Astronomy and Astrophysics, 2016, 585, L1.	2.1	26
65	Geodetic and hydrological aspects of the Merano earthquake of 17 July 2001. Journal of Geodynamics, 2005, 39, 317-336.	0.7	25
66	Inflated flows on Daedalia Planum (Mars)? Clues from a comparative analysis with the Payen volcanic complex (Argentina). Planetary and Space Science, 2009, 57, 556-570.	0.9	25
67	Mercury's geochronology revised by applying Model Production Function to Mariner 10 data: Geological implications. Geophysical Research Letters, 2009, 36, .	1.5	23
68	On the nucleation of non-Andersonian faults along phyllosilicate-rich mylonite belts. Geological Society Special Publication, 2012, 367, 185-199.	0.8	23
69	Sublimation of icy aggregates in the coma of comet 67P/Churyumov–Gerasimenko detected with the OSIRIS cameras on board <i>Rosetta</i> . Monthly Notices of the Royal Astronomical Society, 2016, 462, S57-S66.	1.6	23
70	Geomorphological mapping of comet 67P/Churyumov–Gerasimenko's Southern hemisphere. Monthly Notices of the Royal Astronomical Society, 2016, 462, S573-S592.	1.6	23
71	Mercury Hollows as Remnants of Original Bedrock Materials and Devolatilization Processes: A Spectral Clustering and Geomorphological Analysis. Journal of Geophysical Research E: Planets, 2018, 123, 2365-2379.	1.5	23
72	A three-dimensional modelling of the layered structure of comet 67P/Churyumov-Gerasimenko. Monthly Notices of the Royal Astronomical Society, 2017, 469, S741-S754.	1.6	22

#	Article	IF	CITATIONS
73	Bilobate comet morphology and internal structure controlled by shear deformation. Nature Geoscience, 2019, 12, 157-162.	5.4	22
74	Fluids mobilization in Arabia Terra, Mars: Depth of pressurized reservoir from mounds self-similar clustering. Icarus, 2019, 321, 938-959.	1.1	22
75	Miocene to present major fault linkages through the Adriatic indenter and the Austroalpine—Penninic collisional wedge (Alps of NE Italy). Geological Society Special Publication, 2006, 262, 245-258.	0.8	21
76	Evolution of a poly-deformed relay zone between fault segments in the eastern Southern Alps, Italy. Geological Society Special Publication, 2007, 290, 351-366.	0.8	20
77	Olivine thermal emissivity under extreme temperature ranges: Implication for Mercury surface. Earth and Planetary Science Letters, 2013, 371-372, 252-257.	1.8	20
78	Large-scale fault kinematic analysis in Noctis Labyrinthus (Mars). Planetary and Space Science, 2004, 52, 215-222.	0.9	19
79	Brittle ice shell thickness of Enceladus from fracture distribution analysis. Icarus, 2017, 297, 252-264.	1.1	19
80	The geodynamic evolution of the Italian South Alpine basement from the Ediacaran to the Carboniferous: Was the South Alpine terrane part of the peri-Gondwana arc-forming terranes?. Gondwana Research, 2019, 65, 17-30.	3.0	19
81	Integration of 3D modeling, aerial LiDAR and photogrammetry to study a synsedimentary structure in the Early Jurassic Calcari Grigi (Southern Alps, Italy). European Journal of Remote Sensing, 2015, 48, 527-539.	1.7	17
82	Post-perihelion photometry of dust grains in the coma of 67P Churyumov–Gerasimenko. Monthly Notices of the Royal Astronomical Society, 2017, 469, S195-S203.	1.6	17
83	Mapping and Monitoring Urban Environment through Sentinel-1 SAR Data: A Case Study in the Veneto Region (Italy). ISPRS International Journal of Geo-Information, 2020, 9, 375.	1.4	17
84	THE STEREO CAMERA ON THE BEPICOLOMBO ESA/JAXA MISSION: A NOVEL APPROACH. , 2009, , 305-322.		16
85	In-situ high-temperature emissivity spectra and thermal expansion of C2/c pyroxenes: Implications for the surface of Mercury. American Mineralogist, 2014, 99, 786-792.	0.9	16
86	Self-similar clustering distribution of structural features on Ascraeus Mons (Mars): implications for magma chamber depth. Geological Society Special Publication, 2015, 401, 203-218.	0.8	16
87	Late movement of basin-edge lobate scarps on Mercury. Icarus, 2017, 288, 226-234.	1.1	16
88	Assessment of lithogenic radioactivity in the Euganean Hills magmatic district (NE Italy). Journal of Environmental Radioactivity, 2017, 166, 259-269.	0.9	16
89	Structural Analysis of the Victoria Quadrangle Fault Systems on Mercury: Timing, Geometries, Kinematics, and Relationship with the Highâ€Mg Region. Journal of Geophysical Research E: Planets, 2019, 124, 2543-2562.	1.5	16
90	The assessment of local geological factors for the construction of a Geogenic Radon Potential map using regression kriging. A case study from the Euganean Hills volcanic district (Italy). Science of the Total Environment, 2022, 808, 152064.	3.9	16

#	Article	IF	CITATIONS
91	The Agilkia boulders/pebbles size–frequency distributions: OSIRIS and ROLIS joint observations of 67P surface. Monthly Notices of the Royal Astronomical Society, 2016, 462, S242-S252.	1.6	15
92	Hydrocode simulations of the largest crater on asteroid Lutetia. Planetary and Space Science, 2012, 66, 147-154.	0.9	14
93	Age relationships of the Rembrandt basin and Enterprise Rupes, Mercury. Geological Society Special Publication, 2015, 401, 159-172.	0.8	14
94	Onset of N-Atlantic rifting in the Hoop Fault Complex (SW Barents Sea): An orthorhombic dominated faulting?. Tectonophysics, 2017, 706-707, 59-70.	0.9	14
95	An Integrated Geologic Map of the Rembrandt Basin, on Mercury, as a Starting Point for Stratigraphic Analysis. Remote Sensing, 2020, 12, 3213.	1.8	14
96	Polyphase Tertiary fault kinematics and Quaternary reactivation in the central-eastern Alps (western) Tj ETQq0	О г <u>е</u> ВТ /С)verlgck 10 Tf
97	Estimate of depths of source fluids related to mound fields on Mars. Planetary and Space Science, 2018, 164, 164-173.	0.9	13
98	Dating long thrust systems on Mercury: New clues on the thermal evolution of the planet. Geoscience Frontiers, 2020, 11, 855-870.	4.3	13
99	Time evolution of dust deposits in the Hapi region of comet 67P/Churyumov-Gerasimenko. Astronomy and Astrophysics, 2020, 636, A91.	2.1	13
100	Search for satellites near comet 67P/Churyumov-Gerasimenko using Rosetta/OSIRIS images. Astronomy and Astrophysics, 2015, 583, A19.	2.1	13
101	Thermochronological evidence for a late Pliocene climate-induced erosion rate increase in the Alps. International Journal of Earth Sciences, 2011, 100, 847-859.	0.9	12
102	Modelling of the outburst on 2015 July 29 observed with OSIRIS cameras in the Southern hemisphere of comet 67P/Churyumov–Gerasimenko. Monthly Notices of the Royal Astronomical Society, 2017, 469, S178-S185.	1.6	12
103	Surface Expressions of Subsurface Sediment Mobilization Rooted into a Gas Hydrate-Rich Cryosphere on Mars. Scientific Reports, 2019, 9, 8603.	1.6	12
104	Lateral ramps and strike-slip kinematics on Mercury. Geological Society Special Publication, 2015, 401, 269-290.	0.8	11
105	Are terrestrial plumes from motionless plates analogues to Martian plumes feeding the giant shield volcanoes?. Geological Society Special Publication, 2015, 401, 107-126.	0.8	11
106	Simulations using terrestrial geological analogues to assess interpretability of potential geological features of the Hermean surface restituted by the STereo imaging Camera of the SIMBIOSYS package (BepiColombo mission). Planetary and Space Science, 2008, 56, 1079-1092.	0.9	10
107	Spatial analysis of thickness variability applied to an Early Jurassic carbonate platform in the central Southern Alps (Italy): a tool to unravel synâ€sedimentary faulting. Terra Nova, 2014, 26, 239-246.	0.9	10
108	Influence of the antiformal setting on the kinematics of a large mass movement: the Passo Vallaccia, eastern Italian Alps. Bulletin of Engineering Geology and the Environment, 2011, 70, 497-506.	1.6	9

#	Article	IF	CITATIONS
109	Spectral analysis and geological mapping of the Daedalia Planum lava field (Mars) using OMEGA data. Icarus, 2012, 220, 679-693.	1.1	9
110	Age dating of an extensive thrust system on Mercury: implications for the planet's thermal evolution. Geological Society Special Publication, 2015, 401, 291-311.	0.8	9
111	Multidisciplinary analysis of the Hapi region located on Comet 67P/Churyumov–Gerasimenko. Monthly Notices of the Royal Astronomical Society, 2019, 485, 2139-2154.	1.6	9
112	The Rockyâ€Like Behavior of Cometary Landslides on 67P/Churyumovâ€Gerasimenko. Geophysical Research Letters, 2019, 46, 14336-14346.	1.5	9
113	Geological map of the Middle Triassic Latemar platform (Western Dolomites, Northern Italy). Journal of Maps, 2013, 9, 313-324.	1.0	8
114	A cone on Mercury: Analysis of a residual central peak encircled by an explosive volcanic vent. Planetary and Space Science, 2015, 108, 108-116.	0.9	8
115	Geomorphological and spectrophotometric analysis of Seth's circular niches on comet 67P/Churyumov–Gerasimenko using OSIRIS images. Monthly Notices of the Royal Astronomical Society, 2017, 469, S238-S251.	1.6	8
116	Equatorial grooves distribution on Ganymede: Length and self-similar clustering analysis. Planetary and Space Science, 2021, 195, 105140.	0.9	8
117	Caldera Collapse as the Trigger of Chaos and Fractured Craters on the Moon and Mars. Geophysical Research Letters, 2021, 48, e2021GL092436.	1.5	8
118	Fundamental Science and Engineering Questions in Planetary Cave Exploration. Journal of Geophysical Research E: Planets, 2022, 127, .	1.5	8
119	Geology of the Brenner Pass-Fortezza transect, Italian Eastern Alps. Journal of Maps, 2015, 11, 201-215.	1.0	7
120	The big lobe of 67P/Churyumov–Gerasimenko comet: morphological and spectrophotometric evidences of layering as from OSIRIS data. Monthly Notices of the Royal Astronomical Society, 2018, 479, 1555-1568.	1.6	7
121	Long-term measurements of the erosion and accretion of dust deposits on comet 67P/Churyumov–Gerasimenko with the OSIRIS instrument. Monthly Notices of the Royal Astronomical Society, 2021, 504, 2895-2910.	1.6	7
122	Spectral Units Analysis of Quadrangle H05â€Hokusai on Mercury. Journal of Geophysical Research E: Planets, 2022, 127, .	1.5	7
123	Geology of the Kuiper quadrangle (H06), Mercury. Journal of Maps, 2022, 18, 246-257.	1.0	7
124	How multiple foliations may control large gravitational phenomena: A case study from the Cismon Valley, Eastern Alps, Italy. Geomorphology, 2014, 207, 149-160.	1.1	6
125	An extensional syn-sedimentary structure in the Early Jurassic Trento Platform (Southern Alps, Italy) as analogue of potential hydrocarbon reservoirs developing in rifting-affected carbonate platforms. Marine and Petroleum Geology, 2017, 79, 360-371.	1.5	6
126	Rosetta/OSIRIS observations of the 67P nucleus during the April 2016 flyby: high-resolution spectrophotometry. Astronomy and Astrophysics, 2019, 630, A9.	2.1	6

#	Article	IF	CITATIONS
127	THE â€ [¬] MOON MAPPING' PROJECT TO PROMOTE COOPERATION BETWEEN STUDENTS OF ITALY AND CHINA. International Archives of the Photogrammetry, Remote Sensing and Spatial Information Sciences - ISPRS Archives, 0, XLI-B6, 71-78.	0.2	6
128	ls the Linné impact crater morphology influenced by the rheological layering on the Moon's surface? Insights from numerical modeling. Meteoritics and Planetary Science, 2017, 52, 1388-1411.	0.7	5
129	Global-scale brittle plastic rheology at the cometesimals merging of comet 67P/Churyumov–Gerasimenko. Proceedings of the National Academy of Sciences of the United States of America, 2020, 117, 10181-10187.	3.3	5
130	A New Stereo Algorithm based on Snakes. Photogrammetric Engineering and Remote Sensing, 2011, 77, 495-507.	0.3	4
131	Geomorphology of the El Alamein Battlefield (Southern Front, Egypt). Journal of Maps, 2013, 9, 532-541.	1.0	4
132	Quantitative analysis of isolated boulder fields on comet 67P/Churyumov-Gerasimenko. Astronomy and Astrophysics, 2019, 630, A15.	2.1	4
133	THE â€ [~] MOON MAPPING' PROJECT TO PROMOTE COOPERATION BETWEEN STUDENTS OF ITALY AND CHINA. International Archives of the Photogrammetry, Remote Sensing and Spatial Information Sciences - ISPRS Archives, 0, XLI-B6, 71-78.	0.2	4
134	Rheological and Mechanical Layering of the Crust Underneath Thumbprint Terrains in Arcadia Planitia, Mars. Journal of Geophysical Research E: Planets, 2021, 126, .	1.5	4
135	MEMORIS: a wide angle camera for the BepiColombo mission. Advances in Space Research, 2004, 33, 2182-2188.	1.2	3
136	Pre-Alpine and Alpine deformation at San Pellegrino pass (Dolomites, Italy). Journal of Maps, 2018, 14, 671-679.	1.0	3
137	Slip-tendency analysis as a tool to constrain the mechanical properties of anisotropic rocks. Journal of Structural Geology, 2018, 117, 136-147.	1.0	3
138	3D Extension at Plate Boundaries Accommodated by Interacting Fault Systems. Scientific Reports, 2020, 10, 8669.	1.6	3
139	Geologic Mapping and Age Determinations of Tsiolkovskiy Crater. Remote Sensing, 2021, 13, 3619.	1.8	3
140	Lobate Scarp. , 2015, , 1255-1262.		3
141	Omeonga—A possible large impact structure on the Eastern Kasai Province (D.R. Congo)?. Meteoritics and Planetary Science, 2011, 46, 1804-1813.	0.7	2
142	Geo-structural map of the Laguna Blanca basin (Southern Central Andes, Catamarca, Argentina). Journal of Maps, 2016, 12, 431-442.	1.0	2
143	Spectrophotometric variegation of the layering in comet 67P/Churyumov-Gerasimenko as seen by OSIRIS. Astronomy and Astrophysics, 2019, 630, A16.	2.1	2

#	ARTICLE	IF	CITATIONS
145	Inception and Evolution of La Corona Lava Tube System (Lanzarote, Canary Islands, Spain). Journal of Geophysical Research: Solid Earth, 2022, 127, .	1.4	2
146	Observing Mercury: from Galileo to the stereo camera on the BepiColombo mission. Proceedings of the International Astronomical Union, 2010, 6, 213-218.	0.0	1
147	Correction to "Mercury's geochronology revised by applying Model Production Function to Mariner 10 data: Geological implications― Geophysical Research Letters, 2010, 37, n/a-n/a.	1.5	1
148	Martian Ice Revealed by Modeling of Simple Terraced Crater Formation. Journal of Geophysical Research E: Planets, 2020, 125, e2019JE006108.	1.5	1
149	Geological evolution of the Sinus Iridum basin. Planetary and Space Science, 2020, 194, 105134.	0.9	1
150	Benefits of the Proposed Magia Mission for Lunar Geology. Earth, Moon and Planets, 2010, 107, 267-297.	0.3	0
151	High-Relief Ridge. , 2014, , 1-5.		Ο
152	Strike-Slip Faults. , 2015, , 2069-2078.		0
153	Strike-Slip Faults. , 2014, , 1-12.		Ο
154	Lobate Scarp. , 2014, , 1-11.		0
155	A comet in Alpine style: how standard techniques for the reconstruction of geological structures, pioneered by Émile Argand, can help unravelling the evolution of the Solar System. Rendiconti Online Societa Geologica Italiana, 0, 37, 34-36.	0.3	Ο
156	Small Bodies and Dwarf Planets. , 2018, , 311-343.		0
157	A hidden Oligocene pluton linked to the Periadriatic Fault System beneath the Permian Bressanone pluton, eastern Southern Alps. International Geology Review, 0, , 1-20.	1.1	О